IEEE CSC & ESAS SUPERCONDUCTIVITY NEWS FORUM (global edition), September 2019.
Invited presentation 1-QU-I-1 given at ISEC, 28 July-1 August 2019, Riverside, USA.

High Coherence Quantum Annealing and Fast, High-Fidelity Flux Qubit Readout

Joel Strand, James I. Basham, Jeffrey Grover, Sergey Novikov, Steven Disseler, Zachary Stegen, David G. Ferguson, Alex Marakov, Robert Hinkey, Anthony J. Przybysz, Moe Khalil, Kenneth M. Zick
Advanced Technology Laboratory
Northrop Grumman Corporation
Linthicum, MD, USA
joel.strand@ngc.com

David K. Kim, Alexander Melville, Bethany M. Niedzielski, Jonilyn L. Yoder
MIT Lincoln Laboratory
Lexington, MA, USA

Daniel A. Lidar
University of Southern California
Los Angeles, CA, USA

***Abstract*—Quantum annealing is an interesting candidate for providing a new computing capability for a wide variety of combinatorial optimization problems. We have implemented quantum annealing-capable flux qubits built using MIT Lincoln Laboratory's capacitively-shunted flux qubit fabrication process. These qubits take advantage of lower persistent currents to achieve lower noise sensitivity and increase quantum coherence. Qubits with persistent currents in the nA range present unique challenges for readout, and previous methods using rf-SQUID tunable resonators were too slow for annealing applications. We report on the theory and experimental results of a persistent current readout scheme using quantum flux parametrons as a current amplifier that provides fast, high-fidelity readout of the flux qubit state.**

Keywords—quantum annealing, quantum computing, qubit, coherence, readout

I. INTRODUCTION

Quantum annealing (QA) is an interesting candidate for new computing capability that began as a quantum-inspired classical optimization method in the 1980s [1] and was eventually proposed as a type of analog quantum computing [2][3][4]. The concept of operation typically involves initializing an isolated quantum system, applying analog controls such that the energy landscape represents the classical problem of interest, and then reading out the final state. If the annealing operation is successful, the quantum system will have found the lowest energy state corresponding to the solution to the original problem. In contrast with purely classical annealing, a quantum annealer should be able to take advantage of quantum tunneling to navigate a complex energy landscape and avoid being trapped in local minima.

There are several categories of problems where QA could make significant contributions, such as discrete combinatorial optimization and in sampling applications such as those used in machine learning. For combinatorial optimization, there exist two other quantum approaches to compete with QA: a digital (Trotterized) variant of annealing [5] and the quantum approximate optimization algorithm (QAOA) for use with gate-based quantum computers [6]. QA architectures have much simpler control schemes than gate-based architectures, however, and can reach larger circuit sizes in the near term [7]. They may also be more robust to certain forms of decoherence [8].

II. QUBIT COHERENCE

While QA has not yet demonstrated a speed advantage over classical computing on real-world applications, many important regions of QA design space have yet to be explored. IARPA's Quantum Enhanced Optimization (QEO) program is exploring some of these regions, in particular areas with increased qubit coherence.

The coherence of a quantum system is the time scale over which the system is expected to evolve in a quantum mechanical fashion. The coherence is further defined by two time scales, the relaxation time, T_1, and the dephasing time, T_2. These times are measured with respect to a fixed Hamiltonian, but in QA systems the Hamiltonian is constantly changing during the annealing process, and so it is important to determine the basis in which the decoherence is occurring. Dephasing between energy eigenstates is harmless in QA, but dephasing in the computational basis is fatal to the computation [8]. Dephasing events of the second kind are typically due to thermal population of excited states and happen most often when the temperature of the system is comparable to the energy gaps and when the annealing operation time is comparable to T_1.

Flux qubits [9][10] are a natural choice for implementing QA since the quantum states are characterized by persistent supercurrents flowing in opposite directions, and these currents can be mapped onto the binary spin variable used in QA (Figure 1).

This material is based upon work supported by the Intelligence Advanced Research Projects Activity (IARPA) through the Army Research Office (ARO) Contract No. W911NF-17-C-0050. Any opinions, findings and conclusions or recommendations expressed in this material are those of the author(s) and do not necessarily reflect the views of the Intelligence Advanced Research Projects Activity (IARPA) and the Army Research Office (ARO).

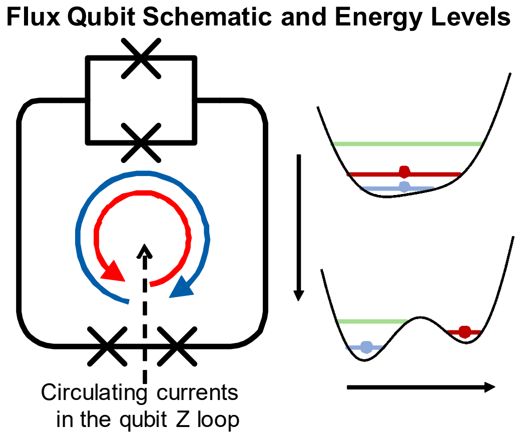

Figure 1 – A schematic of a tunable flux qubit showing the two control fluxes, Φ_X and Φ_Z, and the two persistent current directions corresponding to the ground and excited qubit state. Also shown are representations of the qubit energy potential both before (top) and after (bottom) the annealing operation using Φ_X.

The qubits are first prepared in a state with a single potential well and no persistent current, and during the anneal a double well is created and the direction of the persistent current is determined by the effective bias due to the coupling with neighboring qubits. The coherence time of a flux qubit is strongly dependent on the magnitude of the persistent current (I_p), and scales as $T_1 \sim 1/(I_p)^2$ and $T_2 \sim 1/I_p$ [13][14].

D-Wave Systems has performed much of the pioneering work in this field [11][12], but their work relies on very high persistent currents ($I_p \sim 3\ \mu A$), which severely limits the coherence time of their qubits. This work is performed using capacitively-shunted flux qubits [15] fabricated at MIT Lincoln Laboratory that are designed to have very small persistent currents ($I_p \sim 90\ nA$) and are optimized for long coherence times [16][17].

III. QUBIT READOUT

One of the chief difficulties in using qubits with such small persistent currents is reading out the qubit state at the end of the computation. Previous work with these qubits used a resonator terminated in an rf-SQUID, which acted as a magnetometer to sense the field created by the persistent current in the flux qubit [17]. Modulation of the magnetic flux in the SQUID changed the effective inductance terminating the resonator, which in turn shifted the resonator's frequency (Figure 2). This technique worked well for giving a high-fidelity readout (99.99%), but the resonator had to have a very high quality factor (Q ~ 10,000) in order to avoid detrimental effects on the qubit's coherence, resulting in a very slow readout (~10 µs).

We have since added a new modification to our readout method designed to preserve the high single-shot fidelity but in a much faster timescale. By inserting a Quantum Flux Parametron (QFP) in between the flux qubit and the rf-SQUID resonator (Figure 2), we can amplify the persistent current signal and also isolate the qubit from the resonator [18]. The QFP is very similar in design to the flux qubit, in that it has two flux loops, one controlling the anneal of the energy barrier and one where the persistent current is created, but the energy scale is much larger than that of the flux qubit. The QFP junctions are ten times the size of the flux qubit junctions, with a corresponding increase in the persistent current when it is annealed.

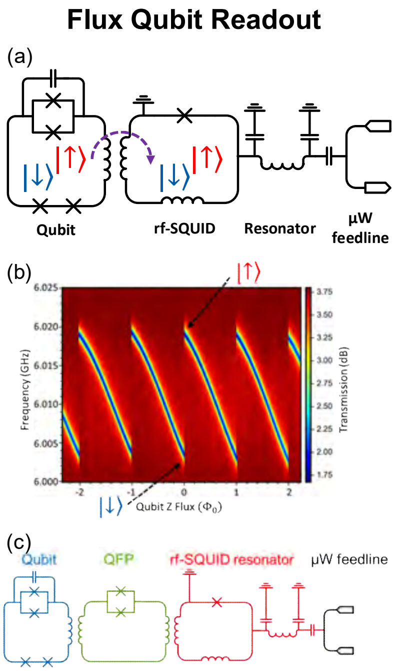

Figure 2 – (a) Schematic of a flux qubit readout method using an rf-SQUID to sense the persistent current in the flux qubit and cause a corresponding shift in the frequency of an attached resonator. (b) Example of resonator transmission data versus probe frequency and qubit Z bias. At integer values of Φ_0 the frequency is extremely sensitive to small changes in persistent current. (c) New schematic that inserts a Quantum Flux Parametron (QFP) between the flux qubit and the rf-SQUID resonator. This acts as a current amplifier and filter to enable faster readout.

The readout operation is performed in several sequential steps (Figure 3). Initially, both the flux qubit and the QFP are in a single-well potential with minimal circulating current. The flux qubit has no X flux bias and only a very small Z bias from neighboring coupled qubits and its local Z control flux, which will determine its final state. The QFP has an X bias of 0.5 Φ_0, which causes the Josephson inductance to diverge and the magnetic susceptibility of the overall loop to go to zero. This is critical because it effectively isolates the flux qubit from the rf-SQUID and readout resonator, allowing us to use a much lower Q resonator without decohering the qubit during the computation phase.

The flux qubit X bias is then ramped to 1 Φ_0, creating a double well potential and projecting the qubit state onto either left or right circulating current. That current creates an effective Z bias on the QFP. Next, the QFP X bias is ramped to 1 Φ_0 and it creates a persistent current whose direction is determined by the flux qubit, but whose amplitude is an order of magnitude larger. The QFP is no longer isolating the qubit from the resonator at this point, but the flux qubit is in a protected classical state at the end of the computation.

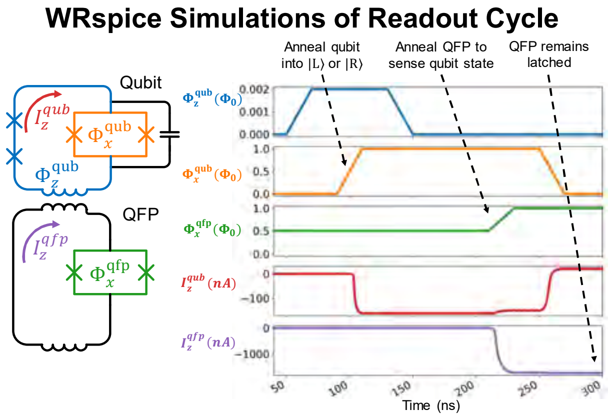

Figure 3 – Schematic of the coupled Flux Qubit/QFP system and WRspice simulations of the annealing process. The flux qubit is initialized with a small Z bias to choose which persistent current state it will end up in, and the QFP has an X bias of 0.5 Φ_0 to make its susceptibility zero and isolate the qubit. The flux qubit and QFP X biases are ramped sequentially to create a final current state in the QFP that is determined by the small initial Z bias on the flux qubit but is an order of magnitude larger than the flux qubit persistent current.

Due to the large persistent currents of the QFP we can use a higher power to probe the resonator frequency, which combined with the relaxation of the constraint on resonator quality factor means that we can read the qubit state much more quickly than before. We were able to perform single-shot readout with 99.9% fidelity in only 90 ns (Figure 4). The anneal of the QFP took 10 ns, and the integration of the resonator signal took 80 ns. We also used this readout technique combined with microwave pulses on the flux qubit to measure the excited state population and track its decay over time. The result was a measurement of $T_1 = 1.58$ µs at a qubit frequency of 4.7 GHz.

IV. DISCUSSION

Quantum annealing offers a potential way to leverage quantum mechanics for computational advantage in devices that can be fabricated and utilized in the near future. In order properties, and developed a fast and high-fidelity readout scheme. By using a QFP as an intermediate filter and amplifier, we achieved 99.9% readout fidelity in only 90 ns, which will dramatically increase the number of computations that can be performed in a given time and open up possibilities for fast feedback.

ACKNOWLEDGMENTS

We thank our Northrop Grumman colleagues for their many contributions; USC and all collaborators on the QEO team; the team at MIT Lincoln Laboratory for very helpful discussions, collaboration, and support, including Steve Weber, Jamie Kerman, George Fitch, Jovi Miloshi, Arjan Sevi, Danna Rosenberg, Gabriel Samach, Cyrus Hirjibehedin, Simon Gustavsson, and William D. Oliver.

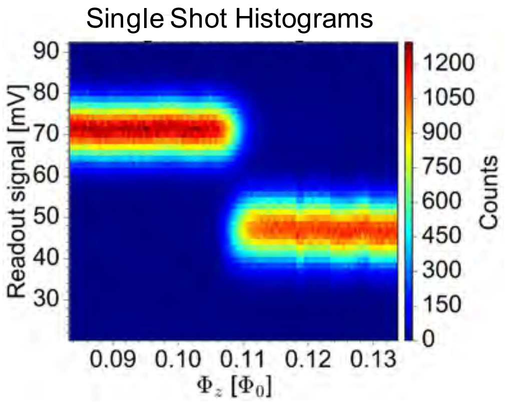

Figure 4 – Histograms of single shot readout events as a function of flux qubit Z bias. The separation was sufficient to achieve 99.9% readout fidelity in 90 ns.

REFERENCES

[1] S. Kirkpatrick, C. D. Gelatt Jr., M. P. Vecchi, "Optimization by Simulated Annealing," *Science,* vol. 220, no. 4598, 1983, pp. 671-680

[2] A. B. Finnila, M. A. Gomez, C. Sebenik, C. Stenson, J. D. Doll, "Quantum Annealing: A new method for minimizing multidimensional functions," *Chem. Phys. Lett.*, vol. 219, no. 5, 1994, pp. 343-348

[3] Tadashi Kadowaki and Hidetoshi Nishimori, "Quantum Annealing in the Transverse Ising Model," *Phys. Rev. E*, vol. 58, no. 5355, 1998

[4] T. Albash and D. A. Lidar, "Adiabatic quantum computation," *Rev. Mod. Phys.* 90, 015002, 2018.

[5] R. Barends et al., "Digitized adiabatic quantum computing with a superconducting circuit," *Nature*, vol. 534, no. 222, 2016.

[6] E. Farhi, J. Goldstone and S. Gutmann, "A quantum approximate optimization algorithm," arXiv:1411.4028, 2014.

[7] Andrew King et al, "Observation of topological phenomena in a programmable lattice of 1,800 qubits," *Nature*, vol. 560, 2018.

[8] T. Albash and D. A. Lidar, "Decoherence in adiabatic quantum computation," *Phys. Rev. A* 91, 062320, 2015.

[9] J. E. Mooij et al., "Josephson persistent-current qubit," *Science*, vol. 285, no. 5430, 1999.

[10] F. G. Paauw, A. Fedorov, C. J. P. M Harmans, and J. E. Mooij, "Tuning the gap of a superconducting flux qubit," *Physical Review Letters*, vol. 102, 090501, 2009.

[11] R. Harris et al., "Experimental demonstration of a robust and scalable flux qubit," *Physical Review B*, vol. 81, no. 13, 134510, 2010.

[12] P. I. Bunyk et al., "Architectural considerations in the design of a superconducting quantum annealing processor," *IEEE Transactions on Applied Superconductivity*, vol. 24, no. 4, pp. 1-10, 2014.

[13] Fei Yan et al, "The flux qubit revisited to enhance coherence and reproducibility," *Nat. Comm.*, vol. 7, no. 12964, 2016

[14] C. M. Quintana et al., "Observation of classical-quantum crossover of 1/f flux noise and its paramagnetic temperature dependence," *Physical Review Letters*, vol. 118, 057702, 2017.

[15] J. S. Birenbaum, "The C-shunt flux qubit: a new generation of superconducting flux qubit", University of California, Berkeley, 2014.

[16] S. J. Weber et al., "Coherent coupled qubits for quantum annealing," *Physical Review Applied,* vol. 8, 014004, 2017.

[17] Sergey Novikov et al, "Exploring More-Coherent Quantum Annealing," *Proc. IEEE Int'l Conf. Rebooting Computing*, 2018.

[18] D.G. Ferguson and A. Przybysz, "Flux Based Readout of a Qubit with Enhanced Isolation from the Environment," US patent application 16/277,560, Feb. 15, 2019.